Journal of Luminescence 197 (2018) 370–375

Contents lists available at ScienceDirect

Journal of Luminescence

journal homepage: www.elsevier.com/locate/jlumin

Photoluminescence tuning and energy transfer process from Tb^{3+} to Eu^{3+} in GPTMS/TEOS–derived organic/silica hybrid films

F.S. de Vicente[a], P. Freddi[a], A.J.G. Otuka[b,*], C.R. Mendonça[b], H.F. Brito[c], L.A.O. Nunes[b], D.R. Vollet[a], D.A. Donatti[a]

[a] Departamento de Física, Universidade Estadual Paulista (Unesp), IGCE, Rio Claro, SP 13506–900, Brazil
[b] Instituto de Física de São Carlos, Universidade de São Paulo, São Carlos, SP 13560–970, Brazil
[c] Instituto de Química, Departamento de Química Fundamental, Universidade de São Paulo, São Paulo, SP 05508-000, Brazil

ABSTRACT

In this work the photoluminescence study and energy transfer from Tb^{3+} to Eu^{3+}–β–diketonate complexes incorporated into organic/Silica hybrid films derived from 3–glycidoxypropyltrimethoxysilane (GPTMS) and tetraethylorthosilicate (TEOS) alkoxysilanes were investigated. Highly homogeneous and transparent films of Ln^{3+}–doped GPTMS/TEOS–derived organic/silica hybrids were obtained from the organic/silica sols prepared by sol–gel. Tb^{3+}:Eu^{3+}–doped GPTMS/TEOS–derived films showed very intense luminescence when excited with UV light. Films co–doped with Tb^{3+} concentration fixed at 40.0×10^{18} ions/cm^3 and Eu^{3+} concentrations of 0, 0.03, 0.05, 0.1, 0.3, 0.5, 1.0, 1.5, and 2.0×10^{18} ions/cm^3 were studied. The films presented characteristic transitions $^5D_4$–$^7F_{6\text{-}3}$ of Tb^{3+} ions and $^5D_0$–$^7F_{0\text{–}4}$ of Eu^{3+} ions measured on the visible spectrum region. Energy transfer from Terbium to Europium was studied through emission decay time measurements of $^5D_4$–$^7F_5$ transition of Tb^{3+} (547 nm) which showed an accentuated decrease (from 1329 to 55 μs) due to the co–doping with Eu^{3+} ions concentrations varied from 0.03 to 1.5×10^{18} ions/cm^3. Energy transfer rate (W_{ET}) of 17.4×10^3 s^{-1} and relative energy transfer efficiency (η_T) of 96% were observed for films samples co–doped with 40×10^{18} ions/cm^3 of Tb^{3+} and 1.5×10^{18} ions/cm^3 of Eu^{3+}. Due to the variation in W_{ET} and η_T from Tb^{3+} to Eu^{3+}, the intensity ratios of Tb^{3+} band at 547 nm ($^5D_4$–$^7F_5$) and Eu^{3+} band at 617 nm ($^5D_0$–$^7F_2$) vary remarkably making the co–doped film samples exhibit different luminescence colors varying from green to orange and red which can be tuned by the Tb^{3+}/Eu^{3+} ratio incorporated into the samples.

1. Introduction

Hybrid materials prepared by combining Silica with various organic species have been attracting growing attention during the last decade. They combine the advantages of organic polymers, like toughness and flexibility, with those of inorganic components such as enhanced mechanical properties, chemical resistance, optical quality, etc. Organic/Silica hybrid materials prepared by sol–gel process are the most studied and important class of hybrids due to their high applicability in several fields such as optics, photonics, energy, and medicine [1–7].

These organic/inorganic hybrids synthesized via sol–gel process consist of a homogenous nanoscale inorganic phase highly dispersed into an organic polymeric matrix due to molecular interactions and covalent linkages achieved during hydrolysis and polycondensation reactions of organically functionalized alkoxysilanes precursors. *Tetraethoxysilane* (TEOS) is a typical compound largely used in sol–gel process owing to its remarkable property of easily converting into silicon dioxide at low temperatures, by formation of Si–O–Si linkages by hydrolysis and polycondensation reactions. The *3–glicidoxypropyltrimethoxysilane* (GPTMS) is an important organically functionalized trialkoxysilane precursor since it possesses functionality of both silicon and a terminal epoxy group in its molecule. GPTMS is commonly employed as coupling agent to strengthen the interaction between organic and inorganic phases because the epoxy ring can be chemically or UV–light opened and activated for molecular bonding [8]. GPTMS has applications in a variety of areas like proton conducting membranes, corrosion and scratch resistant coatings, optical applications, mainly due to its cross linking capacity through the epoxy group.

GPTMS/TEOS–derived organic/silica materials are of high interest, once the resulting hybrid can be tailored to possess the optimal properties and characteristics of each alkoxysilane precursors by varying sol–gel processing parameters. Organic/Silica hybrid films are outstanding materials because through the sol–gel synthesis parameters are possible to control the porosity, refractive index, and thickness of the

* Corresponding author.
E-mail addresses: fabiosv@rc.unesp.br (F.S. de Vicente), otuka@ifsc.usp.br (A.J.G. Otuka).

https://doi.org/10.1016/j.jlumin.2017.12.048
Received 7 June 2017; Received in revised form 13 November 2017; Accepted 22 December 2017
Available online 24 December 2017
0022-2313/

coating and to improve the mechanical properties and transparency of the film without heat treatment [9]. GPTMS/TEOS–derived organic/silica materials present superior mechanical and optical properties compared to TEOS–derived materials [10].

Luminescent lanthanide–doped Organic/Silica hybrid materials have a high potential for different applications such as optical amplifiers, optical waveguides, organic light–emitting diodes (OLEDs) and design of hierarchically–structured Ln^{3+}–containing lamellar hybrids [11–14].

The interest in Tb^{3+} and Eu^{3+} complexes containing organic ligand chromophores is based on the intense and broader absorption bands arising from organic moiety due to absorption cross sections 10^4–10^5 times higher than the Ln^{3+}. These ligands can effectively transfer the absorbed energy to the lanthanides (*antenna effect*) [15,16], yielding very efficient Ln^{3+} complexes with large quantum efficiencies and, consequently, presenting very high luminescence. Lanthanide–based complexes are important in the field of the light–conversion molecular devices (LCMDs) [17]. Ln^{3+} ions form complexes with various organic ligands, such as carboxylic acids, β–diketonates, calixarenes, and heterocyclic systems. In the last decades, many lanthanide–based complexes have been widely investigated as luminescent materials in OLEDs, especially those containing Terbium and Europium [18–23], which possess efficient green (Tb^{3+}) and red (Eu^{3+}) emission colors. Most of the work was focused on lanthanide β–diketonate complexes, because of their good solubility in polymeric matrixes and sol–gel derived organic–inorganic hybrids. Otherwise, most of these compounds are usually achieved as hydrates and consequently the luminescence intensity is quenched due to the activation of non–radiative channels. Besides, the Ln^{3+}–β–diketonate complexes present some limitations such as low thermal stability and poor mechanical properties. The incorporation of Ln^{3+} complexes into organic polymers, liquid crystals and sol–gel derived hybrids has been an efficient alternative in order to improve the characteristics of light emission (e.g. quantum efficiencies, color point tuning) [11–13].

In this work, the photoluminescence study and intermolecular energy transfer from $[Tb(ACAC)_3(H_2O)_3]$ to $[Eu(TTA)_3(H_2O)_2]$ complexes incorporated into GPTMS/TEOS–derived organic/Silica hybrid films obtained by sol–gel process were investigated. Due to the non-radiative energy transfer process from Tb^{3+} to Eu^{3+}, films doped with both complexes exhibit different emission colors varying from green to orange and red, which can be fine-tuned making the Ln^{3+}–doped GPTMS/TEOS efficient luminescent materials. Energy transfer rate (W_{ET}) and relative energy transfer efficiency (η_T) were obtained for films samples co–doped with Tb^{3+} and Eu^{3+} ions.

2. Experimental

2.1. GPTMS/TEOS–derived organic/silica hybrid films preparation

The GPTMS/TEOS–derived organic/Silica hybrid sol was prepared by acid hydrolysis of a mixture (1:1:7:8 mol-%) of *tetraethylorthosilicate* (TEOS) (Aldrich, 99%), *3–glycidoxypropyltrimethoxysilane* (GPTMS) (Aldrich, 98%), deionized water and ethanol (Aldrich, PA). HNO_3 (1 N) was added dropwise until pH 2 (as a catalyst for hydrolysis) and ethanol as a mutual solvent. The hydrolysis was promoted at 80 °C for 2 h under reflux. After cooling down to room temperature, a clear sol of GPTMS/TEOS and very stable against gelation was obtained. Lanthanide complexes $[Eu(TTA)_3(H_2O)_2]$ (TTA: thenoyltrifluoroacetonate) and $[Tb(ACAC)_3(H_2O)_3]$ (ACAC: acetylacetonate) are synthesized are described in Reference [24]. These complexes were used as doping in the obtained sol material. 0.2 g of $[Tb(ACAC)_3(H_2O)_3]$ and 0.01 g of $[Eu(TTA)_3(H_2O)_2]$ were dissolved separately in 5 mL of acetonitrile and calculated volumes of each solution were added to 20 mL of GPTMS/TEOS sol, yielding clear and stable sols doped with Eu^{3+} and Tb^{3+}. To determine the concentration [ions/cm^3] of lanthanides incorporated in the solid hybrid matrix a volume of sol sealed in a plastic container was left ten days inside an oven at 40 °C until gelation. Subsequently, they were left ten more days at 50 °C with a small hole at the container cap for slow drying. Finally, samples removed from the containers were densified at 80 °C/24 h in order to obtain solid monolithic xerogels. Density of 1.396 g/cm^3 was obtained for the monolithic xerogels, measured in deionized water by Archimedes method. Knowing the density and mass of the solid xerogels the lanthanide concentrations (ions/cm^3) incorporated in the solid matrix were determined. For preparation of Tb^{3+}:Eu^{3+}–doped GPTMS/TEOS–derived films, the Ln^{3+} doped sols were deposited with controlled withdraw speed of 10 mm/s by dip–coating onto glass slides in a dry box with nitrogen atmosphere at room temperature. The films were maintained for one hour inside the dry box, after which they were dried in an oven at 80 °C/24 h. In this case, the films were produced with Tb^{3+} concentration of 40×10^{18} ions/cm^3 and Eu^{3+} concentration varying from 0.01 to 1.5 ($\times10^{18}$) ion/cm^3. Tb^{3+}–doped GPTMS/TEOS–derived films (40×10^{18} ions/cm^3) and Eu^{3+}–doped GPTMS/TEOS–derived films (2.0×10^{18} ion/cm^3) were also prepared (Table 1). The as–prepared lanthanide–doped film samples resulted in homogeneous, crack free, well–adherent to the substrates, with high optical quality and transparency. Besides, films exposure to UV irradiation (λ = 350 nm, 450 W), after 6 h of irradiation, exhibit low degradation, indicating significant photostability.

Table 1
Concentrations of Tb^{3+} and Eu^{3+} in 10^{18} ions/cm^3 (and mass %) in the GPTMS/TEOS–derived organic/silica hybrid films.

Ln^{3+}–doped GPTMS/TEOS Films	Tb^{3+}	Eu^{3+}
	10^{18} ions/cm^3 (mass %)	
40Tb–	40(2.0)	–
40Tb–0.03Eu	40	0.03(0.003)
40Tb–0.05Eu	40	0.05(0.005)
40Tb–0.1Eu	40	0.10(0.010)
40Tb–0.3Eu	40	0.30(0.030)
40Tb–0.5Eu	40	0.50(0.050)
40Tb–1.0Eu	40	1.00(0.100)
40Tb–1.5Eu	40	1.50(0.150)
–2.0Eu	–	2.00(0.200)

2.2. Photoluminescence and decay time measurements

Excitation spectra were obtained at room temperature in the visible region, using a He–Cd laser (325 nm – Kimmon IK565) as excitation source. The luminescence signals were dispersed by a monochromator (0.3 m, Thermo Jarrell Ash 82497), detected with a photomultiplier tube (PMT – Hamamatsu R928), and amplified using a lock–in. Decay time measurements were carried out at room temperature using an optical parametric oscillator (OPO – Surelite SLOP/Continuum) pumped by third harmonic from a Nd:YAG laser (355 nm, 5 ns, 10 Hz – Surelite SLII/Continuum).

3. Results and discussion

3.1. Photoluminescence and decay time measurements

For investigating the energy transfer process between $[Tb(ACAC)_3(H_2O)_3]$ and $[Eu(TTA)_3(H_2O)_2]$ complexes incorporated into GPTMS/TEOS–derived organic/silica hybrids, several film compositions were synthesized (Table 1).

Fig. 1 shows the emission spectra of Tb^{3+}–doped GPTMS/TEOS films (40Tb) and Eu^{3+}–doped GPTMS/TEOS films (2.0Eu) excited at 325 nm, recorded at room temperature.

Emission spectra of the 40Tb film consist of emission bands at 491, 547, 587, and 623 nm assigned to the characteristic transitions $^5D_4\rightarrow{}^7F_J$ (J = 6, 5, 4, 3) of Tb^{3+} ion. The most intense green emission of Tb^{3+} is observed at 547 nm ($^5D_4\rightarrow{}^7F_5$). For the 2.0Eu film, the emission spectra

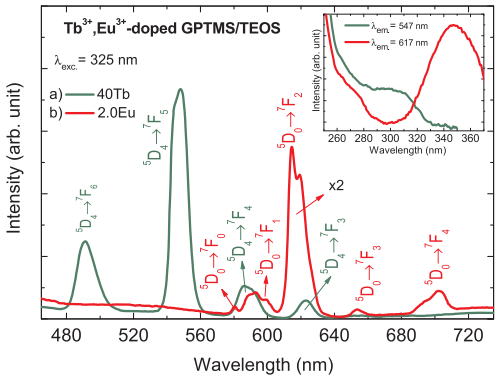

Fig. 1. Emission spectra of the Ln^{3+}–doped GPTMS/TEOS–derived organic/silica hybrid films excited with 325 nm laser line: a) emission spectrum of 40Tb film and b) emission spectrum of 2.0Eu film. The inset shows the excitation spectra for emissions monitored at 547 nm (40Tb) and 617 nm (2.0Eu).

displays bands at 580, 593, 617, 654, and 700 nm assigned to the characteristic transitions $^5D_0 \rightarrow ^7F_J$ (J = 0, 1, 2, 3, 4) of Eu^{3+} ions. The most intense red emission of Eu^{3+} is observed at 617 nm, assigned to the $^5D_0 \rightarrow ^7F_2$ hypersensitive transition. The inset (Fig. 1) shows the excitation spectra obtained for the most intense emission band monitored at 617 nm for the 2.0Eu film, and under emission at 547 nm for the 40Tb film. The excitation spectra reveal broad absorption bands with maxima at 300 and 350 nm due to the energy transfer from TTA and ACAC ligands to Eu^{3+} and Tb^{3+}, respectively.

The emission and excitation spectra of Ln^{3+}-doped organic/Silica films are very comparable with lanthanide complexes [Eu $(TTA)_3(H_2O)_2$] and [Tb$(ACAC)_3.(H_2O)_3$] in solid state, indicating that there is no ligand dissociation or substantial changes in the lanthanide complexes when incorporated in hybrid matrices.

The normalized intensity of luminescence decay curves for 40Tb and 2.0Eu films are presented in Fig. 2. The emission decay curves were well fitted by a single–exponential function:

$$I(t) = I_0 exp(-t/\tau) \quad (1)$$

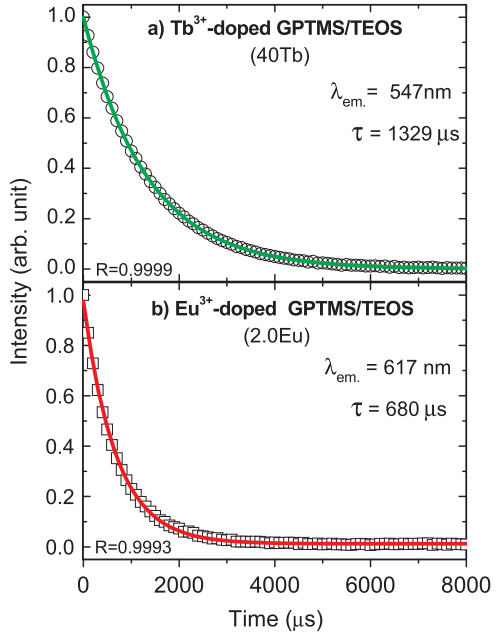

Fig. 2. Luminescence decay curves of the Ln^{3+}–doped GPTMS/TEOS–derived organic/Silica hybrid films excited with 355 nm pulsed laser (5 ns). a) $^5D_4 \rightarrow ^7F_5$ transition (547 nm) of the 40Tb film sample. b) $^5D_0 \rightarrow ^7F_2$ transition (617 nm) of the 2.0Eu film sample. Open symbols are experimental data and solid lines the single–exponential fitting.

where I_0 and $I(t)$ are the luminescence intensities at time 0 and t, respectively, and τ is the luminescence decay lifetime. From the single–exponential fitting, a long luminescence decay lifetime (τ = 1329 μs) was obtained for the most intense Tb^{3+} transition $^5D_4 \rightarrow ^7F_5$ (547 nm) of the 40Tb film sample, and decay lifetime τ = 680 μs for the $^5D_0 \rightarrow ^7F_2$ hypersensitive transition (617 nm) of the 2.0Eu film. The lifetime values obtained for the Tb^{3+} and Eu^{3+} complexes doped into the studied organic/Silica matrix is comparable to the values reported for Tb^{3+} and Eu^{3+} β–diketonate complexes in Zn–based inorganic/organic sol–gel matrix [25], as well as for Tb^{3+} and Eu^{3+} nicotinate complexes in sol–gel silica glasses [26]. Furthermore, the lifetime value (τ = 680 μs) of the 2.0Eu film is comparable to that for the Eu^{3+}β–diketonate complex in Di–Ureasil organic/silica matrix [27]. In addition, studies reveal that the $Eu(TTA)_x$–doped zeolite crystals present a decreasing of the $^5D_0$ non–radiative transition probability after exposure to ammonia gas, showing an increase of lifetime values from 0.41 to 0.62 ms. This effect was attributed to ammonia inducing better shielding of Eu^{3+} ions from luminescence quenchers such as OH groups [28]. In this work we found a lifetime of 0.68 ms for Eu(TTA) incorporated in the GPTMS/TEOS–derived organic/silica hybrid, suggesting that the matrix contributes efficiently against the effect of luminescence quenching, leading to a promising luminescence material to encapsulate Ln^{3+}β–diketonate complexes. Additionally, in our previous work we showed that CdSe/ZnS quantum dots encapsulated in GPTMS/TEOS–derived organic/silica matrix presented higher quantum efficiency than CdSe/ZnS quantum dots suspended in toluene [29].

Fig. 3 shows the emission spectra of the Tb^{3+}:Eu^{3+}–doped GPTMS/TEOS–derived organic/silica hybrid films and the evolution of the emission band intensities as a function of Tb^{3+} and Eu^{3+} concentrations. Measurements were carried out under excitation at 325 nm and at room temperature. It is noteworthy that the luminescence intensities of emission bands assigned to $^5D_4 \rightarrow ^7F_5$ (Tb^{3+}, 547 nm) and to $^5D_0 \rightarrow ^7F_2$ (Eu^{3+}, 617 nm) transitions vary remarkably with the increase of the Europium concentration in the materials. This suggests the occurrence of effective non-radiative energy transfer from Terbium to Europium ions in the co–doped films, since the Tb^{3+} concentration was fixed (Table 1).

In order to understand the changes in the luminescence spectra due to intermolecular energy transfer mechanism, some parameters were evaluated based on the photoluminescence (PL) lifetime decay measurements for the Tb^{3+}:Eu^{3+}–doped GPTMS/TEOS–derived organic/silica hybrid films with different Eu^{3+}concentrations.

Fig. 4 shows the normalized luminescence decay curves of materials using the $^5D_4 \rightarrow ^7F_5$ (Tb^{3+}, 547 nm) transition recorded at room temperature under 5 ns pulse excitation at 355 nm. It is observed a decrease in the lifetime values of Tb^{3+} (donor ion) as the concentration of Eu^{3+} (acceptor ion) is increased in the film.

The increase of the Eu^{3+} concentration modifies significantly the

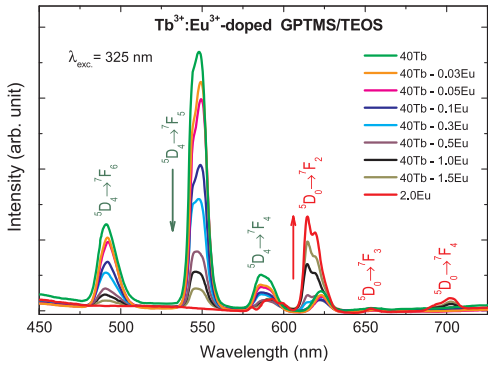

Fig. 3. Emission spectra of the Tb^{3+}:Eu^{3+}–doped GPTMS/TEOS–derived organic/silica hybrid films excited with 325 nm laser line showing the evolution of the bands intensity as a function of Tb^{3+} and Eu^{3+} concentrations.

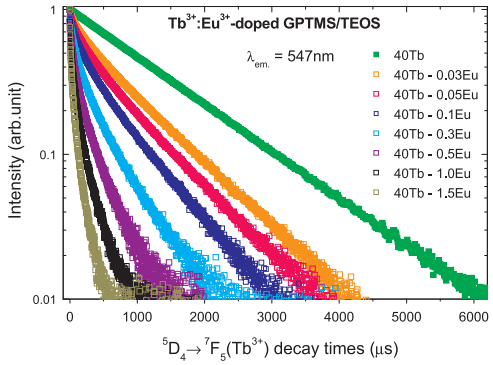

Fig. 4. Normalized luminescence decay curves of Tb^{3+} transition ($^5D_4 \rightarrow {}^7F_5$, 547 nm) for the Tb^{3+}:Eu^{3+}–doped GPTMS/TEOS–derived organic/silica hybrid films excited with 355 nm pulsed laser (5 ns).

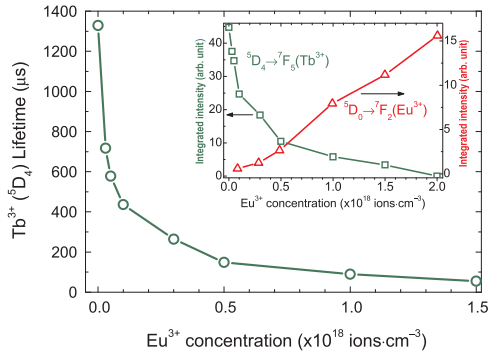

Fig. 5. Lifetime of the $^5D_4$ emitting state of Tb^{3+} ($\tau_{Tb:Eu}$) for the Tb^{3+}:Eu^{3+}–doped GPTMS/TEOS–derived organic/silica hybrid films compositions. Inset shows the integrated intensity for the Tb^{3+} ($^5D_4 \rightarrow {}^7F_5$) and Eu^{3+} ($^5D_0 \rightarrow {}^7F_2$) emission bands as a function of Eu^{3+} concentration.

emission kinetics of the Tb^{3+} ions. The average lifetime ($\tau_{Tb:Eu}$) of Tb^{3+} ($^5D_4$ level) in the presence of Eu^{3+} leads to a deviation from a single–exponential decay due to the energy transfer process, which is calculated by the integral method using:

$$\tau_{Tb:Eu} = \frac{\int_0^\infty I(t).\, tdt}{\int_0^\infty I(t).\, dt} \quad (2)$$

where $I(t)$ is the luminescence intensity at time t. Eq. (2) states that the lifetime is proportional to the area under the normalized decay curve.

The average lifetimes of Tb^{3+} (547 nm) were determined for the Tb^{3+}:Eu^{3+}–doped GPTMS/TEOS–derived films from the luminescence decay curves showed in Fig. 4. The luminescence decay curves (Fig. 4) of the single-doped sample (40Tb film sample) shows a typical long mono-exponential behavior, while on the presence of Eu^{3+} the average lifetime decay of the Tb^{3+} $^5D_4$ emitting state is drastically shortened and deviates from a mono–exponential decay. This result confirms the efficient energy transfer from Tb^{3+} to Eu^{3+} ions [30,31].

The lifetime value of Tb^{3+} (1329 μs) measured in the absence of Eu^{3+} ions (40Tb film sample) drastically dropped from 717 μs (40Tb–0.03Eu) to 55 μs (40Tb–1.5Eu) with increasing the Eu^{3+} concentration in the samples (Table 2). The behavior of the $^5D_4$ emitting state lifetime of Tb^{3+} as a function of the Eu^{3+} concentration in the films is graphically represented in Fig. 5. The integrated intensity for the Tb^{3+} ($^5D_4 \rightarrow {}^7F_5$) and Eu^{3+} ($^5D_0 \rightarrow {}^7F_2$) emission bands as a function of Eu^{3+} concentration is shown in the inset of Fig. 5.

3.2. Energy transfer rates and luminescence color coordinates

Regarding the intermolecular energy transfer mechanism involved in the luminescence spectra, which reflects in the possibility of tuneable color emission, important spectroscopic parameters such as the effective energy transfer rate and the energy transfer efficiency were evaluated by means of the PL lifetime decay measurements. Effective energy transfer rate (W_{ET}) is determined by:

$$W_{ET} = \frac{1}{\tau_{Tb:Eu}} - \frac{1}{\tau_{Tb}} \quad (3)$$

where $\tau_{Tb:Eu}$ and τ_{Tb} are the lifetimes of the $^5D_4$ energy level (Tb^{3+}) in the presence and absence of Eu^{3+} ions, respectively. In addition, the energy transfer efficiency (η_T) is taken into account by:

$$\eta_T = 1 - \frac{\tau_{Tb:Eu}}{\tau_{Tb}} \quad (4)$$

The energy transfer parameters W_{ET} and η_T calculated for the films are presented in Table 2.

Fig. 6 shows the effect of Eu^{3+} concentration on the effective energy transfer rate and energy transfer efficiency for the Tb^{3+}:Eu^{3+}–doped GPTMS/TEOS–derived organic/silica hybrid films compositions. Average lifetime values ($\tau_{Tb:Eu}$) of the $^5D_4$ emitting level of Tb^{3+} ions decrease drastically with the increase of Eu^{3+} concentration from 0 to

Table 2
Lifetime values (τ) of the Tb^{3+} and Eu^{3+} measured for the Tb^{3+}:Eu^{3+}–GPTMS/TEOS–derived organic/silica hybrid films, and the calculated effective energy transfer rate (W_{ET}), and energy transfer efficiency (η_T).

Ln^{3+}–doped GPTMS/TEOS Films	$^5D_4$ (Tb^{3+}) $\tau_{Tb:Eu}$ (μs)	$^5D_0$ (Eu^{3+}) τ_{Eu} (μs)	W_{ET} (10^3 s^{-1})	η_T
40Tb	1329	–	–	
40Tb–0.03Eu	717	–	0.641	0.46
40Tb–0.05Eu	578	–	0.976	0.57
40Tb–0.1Eu	436	–	1.538	0.67
40Tb–0.3Eu	264	–	3.031	0.80
40Tb–0.5Eu	148	–	5.97	0.89
40Tb–1.0Eu	90	–	10.3	0.93
40Tb–1.5Eu	55	–	17.4	0.96
2.0 Eu	–	680	–	

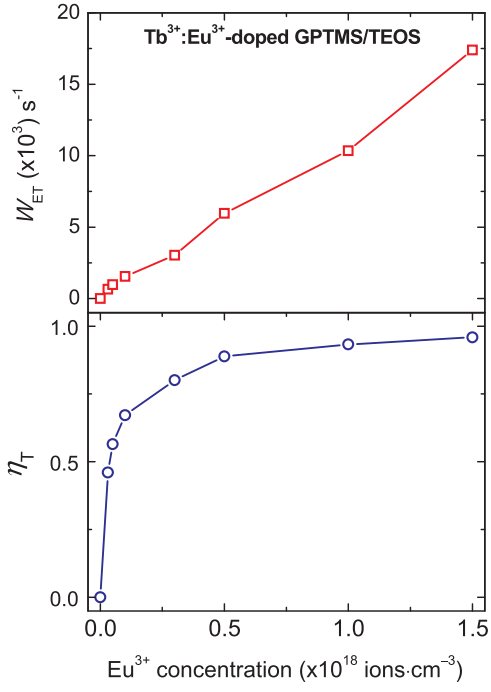

Fig. 6. Effective energy transfer rate (W_{ET}) and energy transfer efficiency (η_T) for the Tb^{3+}:Eu^{3+}–doped GPTMS/TEOS–derived organic/silica hybrid films compositions as a function of Eu^{3+} concentrations.

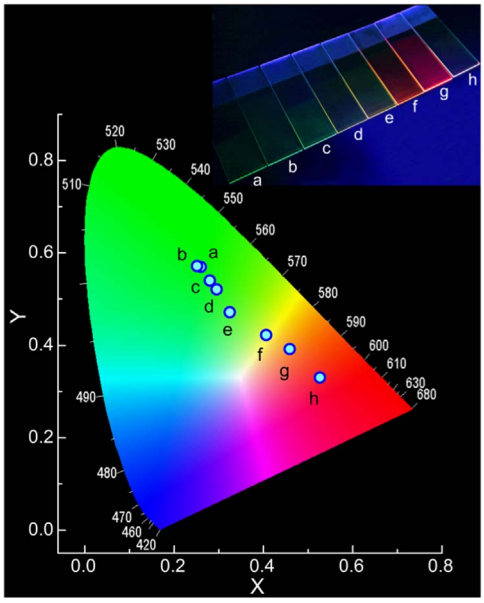

Fig. 7. CIE Chromaticity diagram showing the luminescence coordinates obtained for the Ln^{3+}–doped GPTMS/TEOS–derived organic/silica films: a) 40Tb–0.03Eu, b) 40Tb–0.05Eu, c) 40Tb–0.1Eu, d) 40Tb–0.3Eu, e) 40Tb–0.5Eu, f) 40Tb–1.0Eu, g) 40Tb–1.5Eu, h) 2.0Eu. Inset shows a photograph of the films excited with UV light, exhibiting different photoluminescence colors (from green to red) depending on the Tb^{3+}/Eu^{3+} ratio doped into the films.

1.5×10^{18} ions/cm^3 (Table 2). Associated with $\tau_{Tb:Eu}$ decrease, the W_{ET} value increases till 17.4×10^3 s^{-1} and the relative η_T varied from 46 to 96% with the increase of Eu^{3+}concentration from 0.03 to 1.5×10^{18} ions/cm^3.

These results indicate the existence of an energy transfer pathway which would deactivate the $^5D_4$ emitting state of the Terbium ion. It was found that the energy transfer mechanism takes place efficiently at various concentrations of Eu^{3+} in the Tb^{3+}:Eu^{3+}–doped GPTMS/TEOS–derived organic/silica films. Additionally, this mechanism can be considered more significant for the measured lifetime of Tb^{3+} ion than other factors, such as, natural radiative processes or multiphonon relaxation. The photoluminescence color is a combined result of the two lanthanide luminescent species and the energy transfer mechanism, which depends on the distance between the Eu^{3+}-TTA and Tb^{3+}-ACAC complexes and on the influence of the chemical environment around rare earth ions created by the hybrid organic/silica matrix. Details of the energy transfer process between the Tb^{3+} and Eu^{3+}–β–diketonates, are reported in the reference [24].

Fig. 7 shows the *Commission Internationale de l'Eclairage* (CIE) chromaticity coordinates, calculated from the photoluminescence spectra (Fig. 3) of the lanthanide–doped GPTMS/TEOS–derived organic/silica films. It is observed that when the Eu^{3+} concentration increases, the chromaticity coordinates (x,y) shifted from (0.259, 0.569) for the 40Tb–0.03Eu film to (0.459, 0.392) for the 40Tb–1.5Eu film, corresponding to color tuning from green to orange–red. Moreover, the 2.0Eu film shows color emission with chromaticity coordinates (0.526, 0.330) and much lower emission intensity compared to the films with Tb^{3+}/Eu^{3+}. Film samples present very intense photoluminescence emission when excited by an UV light with irradiance of 2.0 mW/cm^2 onto the samples (see inset Fig. 7).

3.3. Intensity parameters and emission quantum efficiency

The photoluminescence parameters of the Europium ions doped into organic/silica hybrid matrix were obtained analyzing the contributions of the radiative and non-radiative decay rates from the $^5D_0$ emitting level regarding the $^5D_0\rightarrow{}^7F_2$ and $^5D_0\rightarrow{}^7F_4$ transitions of Eu^{3+}.

The emission quantum efficiency of the $^5D_0$ emitting level of the Eu^{3+} ion was determined based on the PL spectrum measured at room temperature for the Eu^{3+}–doped GPTMS/TEOS–derived films (2.0Eu). The experimental intensity parameters Ω_λ (λ = 2 and 4), also known as Judd-Ofelt parameters [32,33], were determined from the ratio between the intensities of the $^5D_0$–^7F_J (J = 2 and 4) and $^5D_0\rightarrow{}^7F_1$ transitions of Eu^{3+} ion [34–36], taking the $^5D_0\rightarrow{}^7F_1$ transition as reference because its intensity is considered insensitive to the ligand environment (predominant magnetic dipole character). The calculations of Ω_λ values were obtained using:

$$A_{0-J} = \frac{4e^2\omega^3}{3\hbar c^3}\frac{1}{2J+1}\chi\sum_{\lambda=2,4}\Omega_\lambda\langle{}^5D_0|U^{(\lambda)}|{}^7F_J\rangle^2, \quad (5)$$

where $\chi = n_0(n_0^2+2)^2/9$ is the Lorentz field correction and the parameters $\langle{}^5D_0|U^{(2)}|{}^7F_2\rangle^2 = 0.0032$ and $\langle{}^5D_0|U^{(4)}|{}^7F_4\rangle^2 = 0.0023$ are the squared reduced matrix elements. The index of refraction has been considered equal to 1.5. The coefficients of spontaneous emission A_{0-J} (J = 2 and 4) were obtained through:

$$A_{0-J} = \left(\frac{\sigma_{0-1}}{S_{0-1}}\right)\left(\frac{S_{0-J}}{\sigma_{0-J}}\right)A_{0-1}, \quad (6)$$

where S_{0-1} and S_{0-J} are related to the area under the emission bands corresponding to the $^5D_0\rightarrow{}^7F_1$ and $^5D_0\rightarrow{}^7F_J$ transitions, respectively. The parameter σ_J is the barycenter of the 0 − J transition and the A_{0-J} is the Einstein´s coefficient for the magnetic dipole transition, with $A_{0-1} \cong 50$ s^{-1}. The lifetime (τ) and the nonradiative (A_{NRAD}) and radiative (A_{RAD}) rates are related through the total decay rate equation $1/\tau = A_{RAD} + A_{NRAD}$, where the A_{RAD} rate was obtained by summing over the radiative rates A_{0-J} for each $^5D_0\rightarrow{}^7F_1$ transition is given by $A_{RAD} = \sum_J A_{0-J}$. Thus, based on the experimental lifetime of the $^5D_0$ emitting level (τ) and A_{RAD} rate, it was possible to determine the nonradiative rates (A_{NRAD}). The emission quantum efficiency of $^5D_0$ emitting level can be determined based on the emission spectra and lifetime measurements, according to:

$$\eta_{Eu} = \frac{A_{RAD}}{A_{RAD} + A_{NRAD}} \quad (7)$$

The GPTMS/TEOS–derived organic/silica hybrid films doped with $[Eu(TTA)_3(H_2O)_2]$ presented higher quantum efficiency than the one measured for the pure $[Eu(TTA)_3(H_2O)_2]$ complex [22] and for the $[Eu(TTA)_3(H_2O)_2]$ complex incorporated into silica particles [36]. Our result is comparable to PMMA films doped with $[Eu(TTA)_3(H_2O)_2]$ β–diketonate complexes [24,37]. Lower values of the intensity parameter Ω_2 indicates that there are small crystal distortions in environment of the site occupied by the Eu^{3+} ion in the GPTMS/TEOS–derived organic/silica matrix compared with the complex $[Eu(TTA)_3(H_2O)_2]$ (see Table 3).

4. Conclusion

GPTMS/TEOS–derived organic/silica hybrid films obtained by

Table 3
Experimental intensity parameters ($\Omega_{2,4}$), radiative (A_{RAD}) and non-radiative (A_{NRAD}) rates, lifetimes of the $^5D_0$ emitting level(s) (τ) and emission quantum efficiencies (η) for the Eu^{3+}– doped GPTMS/TEOS Films compared to Eu^{3+} systems.

Luminescence materials	Ω_2 (10^{-20} cm^2)	Ω_4 (10^{-20} cm^2)	A_{RAD} (s^{-1})	A_{NRAD} (s^{-1})	τ (ms)	η (%)
Eu^{3+}– doped GPTMS/TEOS	10	5	582	889	0.68	40
$[Eu(TTA)_3(H_2O)_2]$[a]	33	5	1110	2736	0.30	29
PMMA:1%$Eu(TTA)_3$[b]	43	10	1482	1788	0.31	45

[a] [22] and.
[b] [24].

sol–gel synthesis doped with $[Tb(ACAC)_3(H_2O)_3]$ and $[Eu(TTA)_3(H_2O)_2]$ complexes were successfully produced. The doped films deposited by dip–coating onto glass slides are highly homogeneous, crack–free and colorless, with high transparency in the visible. The GPTMS/TEOS–derived organic/silica hybrid is an excellent matrix to incorporate Eu^{3+} and Tb^{3+} organic complexes, yielding film samples with outstanding optical properties associated with good mechanical properties, such as scratch resistant layers. The Tb^{3+}:Eu^{3+}–doped GPTMS/TEOS–derived hybrid films showed very intense photoluminescence when excited at the UV, from the transitions $^5D_4 \rightarrow {}^7F_{6\text{-}3}$ of Tb^{3+} and $^5D_0 \rightarrow {}^7F_{0\text{–}4}$ of Eu^{3+} and high radiative rate decays. These effects are due to the intense absorption bands of the organic ligands with effective energy transfer to the lanthanides (antenna effect). The Organic/Silica Hybrid films doped with Tb^{3+} and Eu^{3+} showed efficient energy transfer from Terbium to Europium ions, with relative energy transfer efficiency (η_T) of 96% and energy transfer rate (W_{ET}) of $17.4 \times 10^3\ s^{-1}$ for samples co–doped with 40×10^{18} ions/cm^3 of Tb^{3+} and 1.5×10^{18} ions/cm^3 of Eu^{3+}. The color and intensity of the luminescence can be controlled varying the ions ratio incorporated in the samples. Intensity of Tb^{3+} band at 547 nm ($^5D_4 \rightarrow {}^7F_5$) and Eu^{3+} band at 617 nm ($^5D_0 \rightarrow {}^7F_2$) vary remarkably due to the variation in the energy transfer efficiencies W_{ET} and η_T, making the co–doped samples exhibit different luminescence colors varying from green to orange and red.

Acknowledgements

The authors are thankful to the Brazilian funding agencies, Grant #2016/20094-8, São Paulo Research Foundation (FAPESP), Coordination for the Improvement of Higher Education Personnel (CAPES), National Council for Scientific and Technological Development (CNPq), and Fundação para o Desenvolvimento da Unesp (FUNDUNESP) for the financial support for this work.

References

[1] C.J. Brinker, G.W. Scherer, Sol-Gel Science: The Physics and Chemistry of Sol-Gel Processing, Academic Press, 1990.
[2] R.W. Jones, Fundamental Principles of Sol-Gel Technology, Institute of Metals, 1989.
[3] L.M.G. Abegao, D.S. Manoel, A.J.G. Otuka, P.H.D. Ferreira, D.R. Vollet, D.A. Donatti, L. De Boni, C.R. Mendonca, F.S. De Vicente, J.J. Rodrigues, M. Alencar, Random laser emission from a Rhodamine B-doped GPTS/TEOS-derived organic/silica monolithic xerogel, Laser Phys. Lett. 14 (6) (2017) 065801–065806.
[4] P.H.D. Ferreira, A.J.G. Otuka, E.C. Barbano, D.S. Manoel, F.S. De Vicente, D.R. Vollet, D.A. Donatti, L. Misoguti, C.R. Mendonca, Femtosecond laser fabrication of waveguides in Rhodamine B-doped GPTS/TEOS-derived organic/silica monolithic xerogel, Opt. Mater. 47 (2015) 310–314.
[5] M. Mihelcic, V. Francetic, J. Kovac, A.S. Vuk, B. Orel, R. Kunic, D. Peros, Novel sol-gel based selective coatings: from coil absorber coating to high power coating, Sol. Energy Mater. Sol. Cells 140 (2015) 232–248.
[6] J. Stergar, U. Maver, Review of aerogel-based materials in biomedical applications, J. Sol-Gel Sci. Technol. 77 (3) (2016) 738–752.
[7] X.X. Zhang, W.J. Zhang, Y.J. Li, C.L. Li, Hybrid luminescent materials of graphene oxide and rare-earth complexes with stronger luminescence intensity and better thermal stability, Dyes Pigm. 140 (2017) 150–156.
[8] M.A. Robertson, R.A. Rudkin, D. Parsonage, A. Atkinson, Mechanical and thermal properties of organic/inorganic hybrid coatings, J. Sol-Gel Sci. Technol. 26 (1–3) (2003) 291–295.
[9] Y. Sorek, R. Reisfeld, A.M. Weiss, Effect of composition and morphology on the spectral properties and stability of dyes doped in a sol-gel glass waveguide, Chem. Phys. Lett. 244 (5–6) (1995) 371–378.
[10] P. Innocenzi, C. Figus, T. Kidchob, M. Valentini, B. Alonso, M. Takahashi, Sol-gel reactions of 3-glycidoxypropyltrimethoxysilane in a highly basic aqueous solution, Dalton Trans. 42 (2009) 9146–9152.
[11] K. Binnemans, Lanthanide-based luminescent hybrid materials, Chem. Rev. 109 (9) (2009) 4283–4374.
[12] S.S. Nobre, C.D.S. Brites, R.A.S. Ferreira, V.D. Bermudez, C. Carcel, J.J.E. Moreau, J. Rocha, M.W.C. Man, L.D. Carlos, Photoluminescence of Eu(III)-doped lamellar bridged silsesquioxanes self-templated through a hydrogen bonding array, J. Mater. Chem. 18 (35) (2008) 4172–4182.
[13] L.D. Carlos, R.A.S. Ferreira, V.D. Bermudez, S.J.L. Ribeiro, Lanthanide-containing light-emitting organic-inorganic hybrids: a bet on the future, Adv. Mater. 21 (5) (2009) 509–534.
[14] J.J.E. Moreau, L. Vellutini, M.W.C. Man, C. Bied, J.L. Bantignies, P. Dieudonne, J.L. Sauvajol, Self-organized hybrid silica with long-range ordered lamellar structure, J. Am. Chem. Soc. 123 (32) (2001) 7957–7958.
[15] E. DeOliveira, C.R. Neri, O.A. Serra, A.G.S. Prado, Antenna effect in highly luminescent Eu^{3+} anchored in hexagonal mesoporous silica, Chem. Mater. 19 (22) (2007) 5437–5442.
[16] F.P. Aguiar, I.F. Costa, J.G.P. Espinola, W.M. Faustino, J.L. Moura, H.F. Brito, T.B. Paolini, M.C.F.C. Felinto, E.E.S. Teotonio, Luminescent hybrid materials functionalized with lanthanide ethylenodiaminotetraacetate complexes containing beta-diketonate as antenna ligands, J. Lumin. 170 (2016) 538–546.
[17] R. Pavithran, N.S.S. Kumar, S. Biju, M.L.P. Reddy, S.A. Junior, R.O. Freire, 3-phenyl-4-benzoyl-5-isoxazolonate complex of Eu^{3+} with tri-n-octylphosphine oxide as a promising light-conversion molecular device, Inorg. Chem. 45 (5) (2006) 2184–2192.
[18] J. Kido, K. Nagai, Y. Ohashi, Electroluminescence in a terbium complex, Chem. Lett. 4 (1990) 657–660.
[19] A. Edwards, C. Claude, I. Sokolik, T.Y. Chu, Y. Okamoto, R. Dorsinville, Photoluminescence and electroluminescence of new lanthanide-(methoxybenzoyl) benzoate complexes, J. Appl. Phys. 82 (4) (1997) 1841–1846.
[20] X.C. Gao, H. Cao, C.H. Huang, B.G. Li, S. Umitani, Electroluminescence of a novel terbium complex, Appl. Phys. Lett. 72 (18) (1998) 2217–2219.
[21] Y. Kawamura, Y. Wada, M. Iwamuro, T. Kitamura, S. Yanagida, Near-infrared electroluminescence from ytterbium(III) complex, Chem. Lett. 3 (2000) 280–281.
[22] E.E.S. Teotonio, H.F. Brito, M.C.F.C. Felinto, C.A. Kodaira, O.L. Malta, Luminescence investigations on Eu(III) thenoyltrifluoroacetonate complexes with amide ligands, J. Coord. Chem. 56 (10) (2003) 913–921.
[23] C. Molina, K. Dahmouche, Y. Messaddeq, S.J.L. Ribeiro, M.A.P. Silva, V.D. Bermudez, L.D. Carlos, Enhanced emission from Eu(III) beta-diketone complex combined with ether-type oxygen atoms of di-ureasil organic-inorganic hybrids, J. Lumin. 104 (1–2) (2003) 93–101.
[24] J.A. Kai, M.C.F.C. Felinto, L.A.O. Nunes, O.L. Malta, H.F. Brito, Intermolecular energy transfer and photostability of luminescence-tuneable multicolour PMMA films doped with lanthanide-β-diketonate complexes, J. Mater. Chem. 21 (11) (2011) 3796–3802.
[25] R.F. Martins, R.F. Silva, R.R. Goncalves, O.A. Serra, Luminescence in colorless, transparent, thermally stable thin films of Eu^{3+} and Tb^{3+} β-diketonates in hybrid inorganic-organic zinc-based sol-gel matrix, J. Fluoresc. 20 (3) (2010) 739–743.
[26] P. Lenaerts, C. Gorller-Walrand, K. Binnemans, Luminescent europium(III) and terbium(III) nicotinate complexes covalently linked to a 1,10-phenanthroline functionalised sol-gel glass, J. Lumin. 117 (2) (2006) 163–169.
[27] M. Fernandes, V.D. Bermudez, R.A.S. Ferreira, L.D. Carlos, N.V. Martins, Incorporation of the $Eu(tta)_3(H_2O)_2$ complex into a co-condensed d-U(600)/d-U (900) matrix, J. Lumin. 128 (2) (2008) 205–212.
[28] Y.X. Ding, Y.G. Wang, H.R. Li, Z.Y. Duan, H.H. Zhang, Y.X. Zheng, Photostable and efficient red-emitters based on zeolite L crystals, J. Mater. Chem. 21 (38) (2011) 14755–14759.
[29] L.D.S. Alencar, V. Pilla, A.A. Andrade, D.A. Donatti, D.R. Vollet, F.S. De Vicente, High fluorescence quantum efficiency of CdSe/ZnS quantum dots embedded in GPTS/TEOS-derived organic/silica hybrid colloids, Chem. Phys. Lett. 599 (2014) 63–67.
[30] J.Y. Park, H.C. Jung, G.S.R. Raju, B.K. Moon, J.H. Jeong, J.H. Kim, Tunable luminescence and energy transfer process between Tb^{3+} and Eu^{3+} in GYAG:Bi^{3+}, Tb^{3+}, Eu^{3+} phosphors, Solid State Sci. 12 (5) (2010) 719–724.
[31] Y.C. Jia, Y.J. Huang, Y.H. Zheng, N. Guo, H. Qiao, Q. Zhao, W.Z. Lv, H.P. You, Color point tuning of $Y_3Al_5O_{12}$:Ce^{3+} phosphor via Mn^{2+}-Si^{4+} incorporation for white light generation, J. Mater. Chem. 22 (30) (2012) 15146–15152.
[32] B.R. Judd, Optical absorption intensities of rare-earth ions, Phys. Rev. 127 (3) (1962) 750–761.
[33] G.S. Ofelt, Intensities of crystal spectra of rare-earth ions, J. Chem. Phys. 37 (3) (1962) 511–520.
[34] H.F. Brito, O.L. Malta, M.C.F.C. Felinto, E.E.S. Teotoni, Luminescence Phenomena Involving Metal Enolates, in PATAI'S Chemistry of Functional Groups, John Wiley & Sons, Ltd., 2009.
[35] O.L. Malta, H.F. Brito, J.F.S. Menezes, F. Silva, S. Alves, F.S. Farias, A.V.M. deAndrade, Spectroscopic properties of a new light-converting device Eu (thenoyltrifluoroacetonate)$_3$ 2(dibenzyl sulfoxide). A theoretical analysis based on structural data obtained from a sparkle model, J. Lumin. 75 (3) (1997) 255–268.
[36] A.V.S. Lourenco, C.A. Kodaira, E.M. Ramos-Sanchez, M.C.F.C. Felinto, H. Goto, M. Gidlund, O.L. Malta, H.F. Brito, Luminescent material based on the Eu $(TTA)_3(H_2O)_2$ complex incorporated into modified silica particles for biological applications, J. Inorg. Biochem. 123 (2013) 11–17.
[37] E.B. Gibelli, J. Kai, E.E.S. Teotonio, O.L. Malta, M.C.F.C. Felinto, H.F. Brito, Photoluminescent PMMA polymer films doped with Eu^{3+}-beta-diketonate crown ether complex, J. Photochem. Photobiol. A-Chem. 251 (2013) 154–159.